12. FE MODELLING OF COMPOSITE BEAM

12.1 PREAMBLE

One of the most common composite systems is the composite beam, in which steel beams interact with concrete slab at supports by means of shear connectors. The connection system generally permits a relative slip between the lower fiber of the concrete slab and upper fiber of the beam. Flexibility of the connection system influences the structural response for each load level at both ultimate and serviceability limit state. In addition, creep and shrinkage of concrete affect the structural response under long term loading. To consider this several numerical algorithm based on either finite difference method or finite element methods have been proposed by researchers. Many simple and computationally less demanding approaches based on one dimensional modelling have been described in the literature by Amadio and Fragiacomo [49], Salari et al. [111] and Ayoub and Filippou [112]. All the nonlinear models take into account the connection flexibility. Current regulations given by Eurocode 4 [7] permit the use of the both full and partial connection system. The behavior of headed shear connector in composite beam has been studied by El-Lobody and Lam [76] using FEM. Study of full and partial connection in composite beams has been carried out by Queiroz et al. [78] which covers load defection behavior, longitudinal slip at steel-concrete interface, distribution of stud shear force and failure mode. Three dimensional FE models can cover many features, including the detection of local aspect of behavior accurately but two dimensional models could be better option for generation of the result for more complex structural system due to numerical convergence aspect and processing time.

Here the behavior of a simply supported composite beam is modelled using ANSYS software under static concentrated and distributed loads. Detailed parametric study is carried using the finite element method and results are compared with the available experimental results to confirm the proposed 2D modelling aspects.

12.2 ELEMENTS SELECTED

The element types selected from the ANSYS library for modelling of composite beam shown in **Fig. 12.1** are as follows:

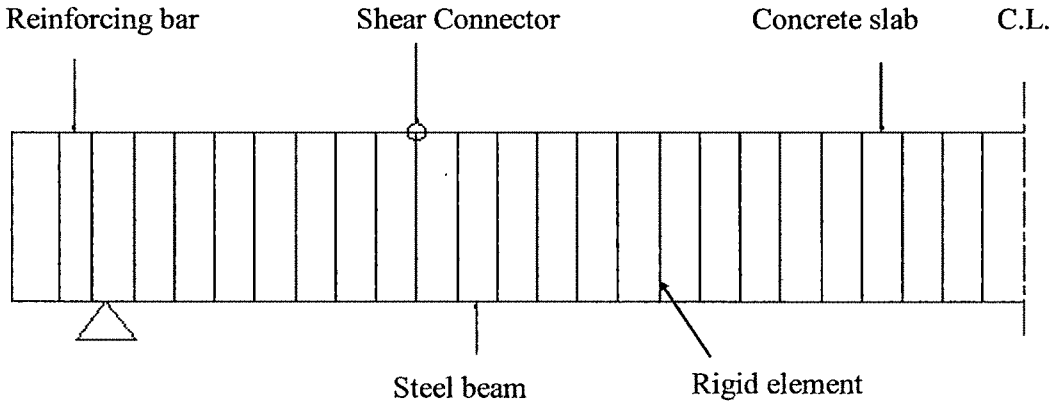

Fig. 12.1 Finite Element Types used in a General Structural Arrangement

BEAM23 - It is a two-dimensional plastic beam element. Concrete slab and steel beam are modeled by it.

LINK1 - It is a two dimensional plastic bar element. Reinforcing bars and the steel connection components are modeled by it.

COMBIN39 - It is a nonlinear spring element which is used to model the shear connectors.

BEAM3 - It is a two dimensional elastic beam element which is used to simulate a rigid region between the node that defines the shear connector element and the node that defines the steel beam element, in order to guarantee that the rotation of the section remains the same over the full composite beam depth.

12.3 MATERIAL PROPERTIES

12.3.1 MATERIAL MODEL OF CONCRETE

The uniaxial behavior of concrete is assumed which is described by a piece-wise linear total stress- total strain curve, starting at the origin. It has positive stress and strain values, considering the concrete compressive strength (f_c) corresponding to a compressive strain of 0.2%. To avoid numerical problems due to unrestricted flow, assumption is made that corresponding to 0.35% concrete strain a total increase of 0.05 N/mm^2 in the compressive strength takes place.

For modelling multilinear isotropic hardening, Von Mises yield criterion coupled with isotropic work hardening is assumed. The actual cylinder strength test value is taken as the concrete slab compressive strength. The concrete tensile strength and the Poisson's ratio are assumed 1/10th of its compressive strength and 0.2 respectively. The elastic modulus is evaluated as per Eurocode 4 considering $\gamma_c = 24$ kN/m^3 in the following formula

$$E_c = 9500(f_c + 8)^{1/3}\left(\gamma_c/_{24}\right)^{1/2} \quad \ldots(12.1)$$

The concrete element shear transfer coefficients considered are 0.2 for open crack and 0.6 for closed crack. For stress relaxation coefficient the default value of 0.6 is used. For improving the convergence the crushing capability of the concrete element is disabled.

12.3.2 Material Model of Shear Connectors

The shear connectors are represented by the nonlinear spring elements. The load-slip data is required as input for representing connectors. The data available from the empirical formulations or curves obtained directly from the available push-off tests can be utilized.

12.3.3 Material Model of Steel Beam

The multilinear work-hardening property using Von Mises criterion with isotropic hardening is used to model the steel beam. The stress-strain relationship is linearly elastic upto yielding, perfectly plastic between the elastic limit (ε_y) and the beginning of strain hardening. For the strain hardening branch it follows the constitutive law suggested by Gattesco [44].

$$\sigma = f_y + E_h(\epsilon - \epsilon_h)\left(1 - E_h\frac{\epsilon - \epsilon_h}{4(f_u - f_y)}\right) \quad \ldots(12.2)$$

where f_y and f_u are the yield and ultimate tensile stresses of the steel component respectively; E_h and ε_h are the strain hardening modulus and strain at the strain hardening of the steel component respectively.

12.3.4 Material Model of Reinforcing Bars

All tensile forces are balanced by the steel in cracked cross-section. In between the adjacent cracks, tensile forces are transmitted from steel to the surrounding concrete by bond forces. The tension stiffening effect is taken into account which can be defined as the increase in the stiffness of the tensile reinforcement due to the contribution of concrete in tension between cracks. Therefore, the stress-strain relationship for the embedded reinforcement provides a higher stiffness and a lower overall ductility than for the reinforcement alone.

Hanswille [41] proposed a model to take into account the tension-stiffening effect. **Figure 12.2** depicts a simplified relationship for embedded reinforcing steel bar. In **Fig. 12.2**, σ_{sr1}= first crack stress in the steel, σ_s = stress in reinforcement, f_{ys} = yield stress of reinforcement, f_t = tensile strength of reinforcement, N_s = normal force on the cracked reinforced concrete slab, A_s = area of reinforcement, β_t = 0.40 for short-term loading, ε_{ys} = strain of reinforcement at the yield point, ε_{smu} = ultimate strain of embedded reinforcement, ε_{su} = characteristics elongation of bare reinforcement at maximum load and $\Delta\varepsilon_{sr}$= increase of steel strain in the cracking state.

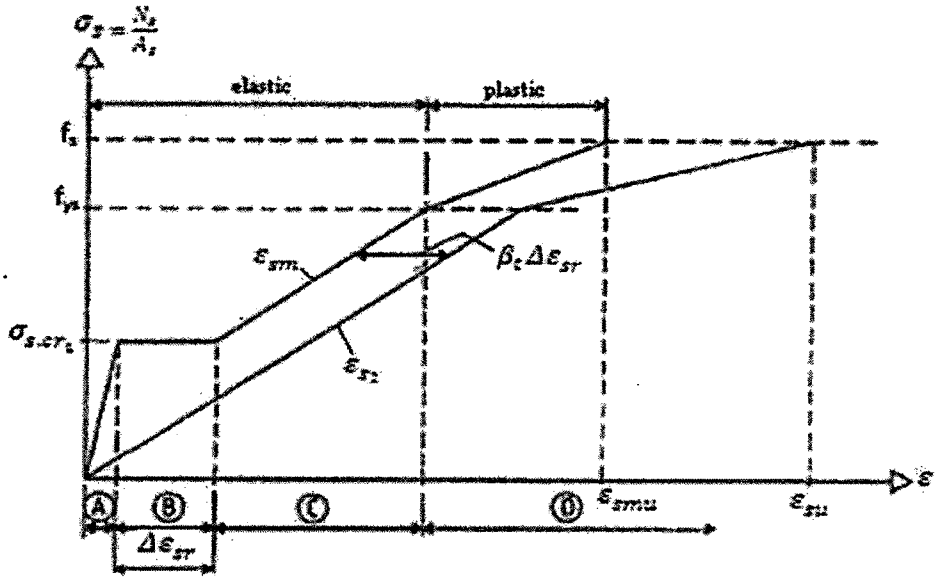

Fig. 12.2 Simplified Stress-Strain Relationship for Embedded Reinforcing Steel

12.4 FAILURE CRITERION

To define the ultimate load for each numerical investigation two limits are established, lower and upper bound, corresponding to concrete compressive strains of 0.2% and 0.35% respectively. These two limits define an interval in which the composite beam collapse load is located. A third limit condition can also be reached when the beam's most heavily loaded stud reaches its ultimate load. If the stud failure is located below the lower bound for concrete failure, the mode is taken as stud failure. If the stud failure point is located beyond the upper bound of concrete failure, the mode of failure is taken as concrete crushing. In the intermediate case, where the stud failure point lies between the bounds of concrete failure, the mode of failure could be either.

12.5 VALIDATION OF MODEL – SS BEAM EXAMPLE

Chapman and Balakrishnan [14] investigated the behavior of seventeen solid simply supported composite T-beams under static concentrated and distributed loading applied on the axis of the beam. The I-shaped steel beam spanning 5490 mm was considered by them with depth as 305 mm and concrete slab of size 152 mm thick x 1220 mm wide. The number and type of studs as well as steel and concrete strength were varied according to the tested composite beam. The slab was reinforced with four top and four bottom 8 mm bars. The transverse reinforcement had top and bottom bars of 12.7 mm @ 152 mm c/c and 12.7 mm @ 305 c/c respectively. **Figure 12.3** shows the layout of the simply supported beam.

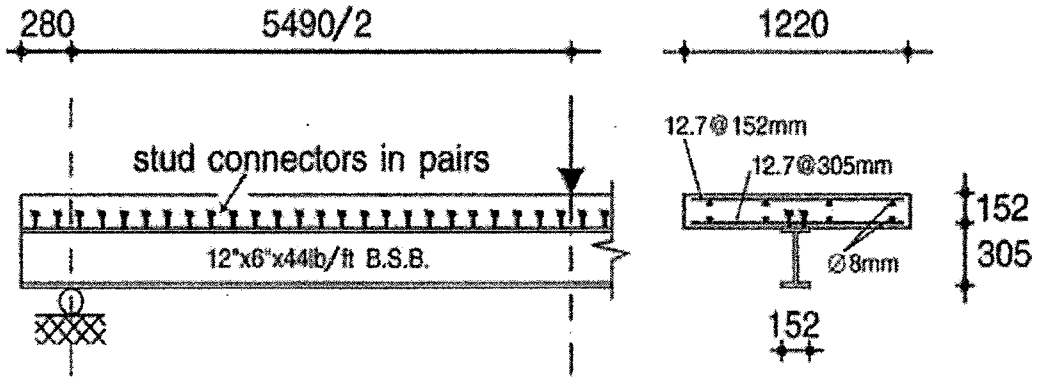

Fig. 12.3 Simply Supported Beam Layout

Table 12.1 gives the detail of the composite beams tested by Chapman and Balakrishnan. The studs having diameter 12.7 mm, height 50 mm and placed at 121 mm c/c were used in beam E1. The loading pattern considered was midspan concentrated. While in beam U4 stud having the dimension of diameter as 19 mm and height as 102 mm were considered. The triangular spacing has been considered along with the uniformly distributed load.

The results obtained using the present 2D model are compared with the experimental data given by Chapman et al. [14] and the numerical results based on 3D FE analysis given by Queiroz et al. [78].

Table 12.1 Details of Composite Beams Tested by Chapman and Balakrishnan

Beam Designation		A2	A3	A4	A5	A6	B1	C1	D1	E1	U1	U3	U4
Stud Diameter (mm)	19	√	√	√	√	√	√	√			√	√	√
	12.7								√	√			
Stud Overall Length (mm)	102	√	√	√	√	√			√		√	√	√
	76						√						
	50							√		√			
Number Of Studs	100								√	√			
	76	√											
	68		√										
	56			√							√	√	
	44				√		√	√					
	32					√							√
Spacing in Pairs (mm)	121								√	√			a
	159	√											a
	178		√										a
	216			√							√	√	a
	274				√		√	√					a
	378					√							a
Mode of Failure	Slab Crushing	√	√	√	√		√	√	√	√	√	√	
	Stud Failure					√							√
Load Type		Mid Span Concentrated Load									UDL		

a – Triangular Spacing

The load- midspan deflection curves shown in **Figs. 12.4** and **12.5** for the beams U4 and E1 respectively show good agreement with the experimental and numerical results. The slip at the steel-concrete interface along the axis for the cases E1 and U4 is plotted in **Figs. 12.6** and **12.7** respectively. In these figures X indicates section position from the left support, L represents the total beam length and slip is plotted at ultimate load.

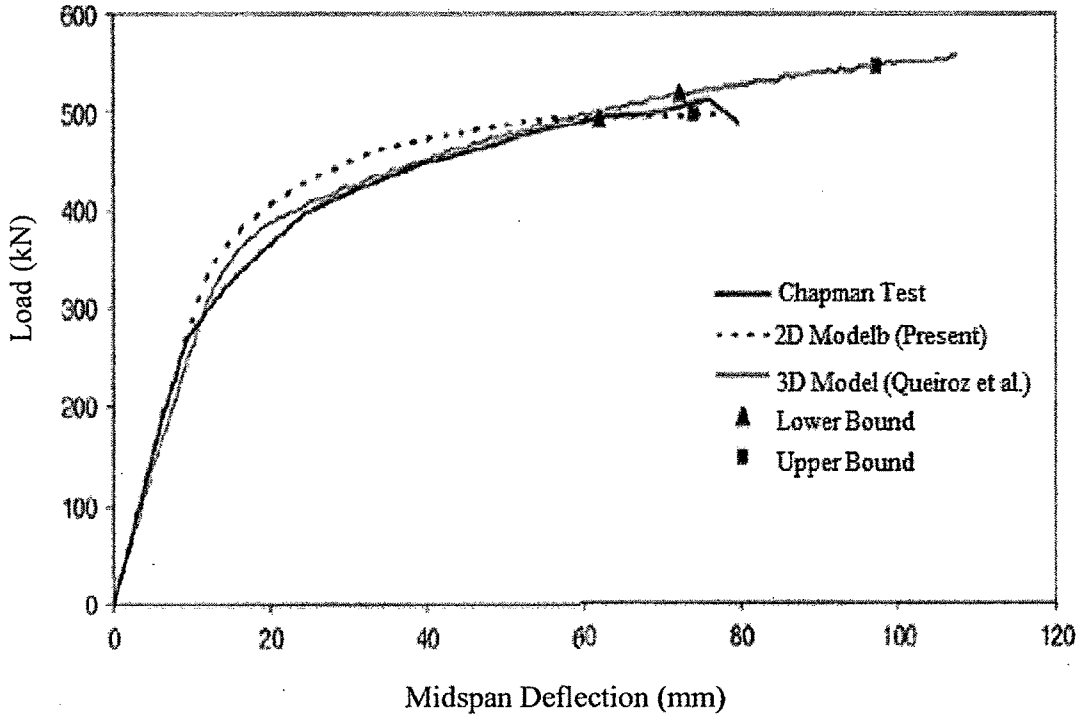

Fig. 12.4 Load versus Mid Span Deflection for Beam E1

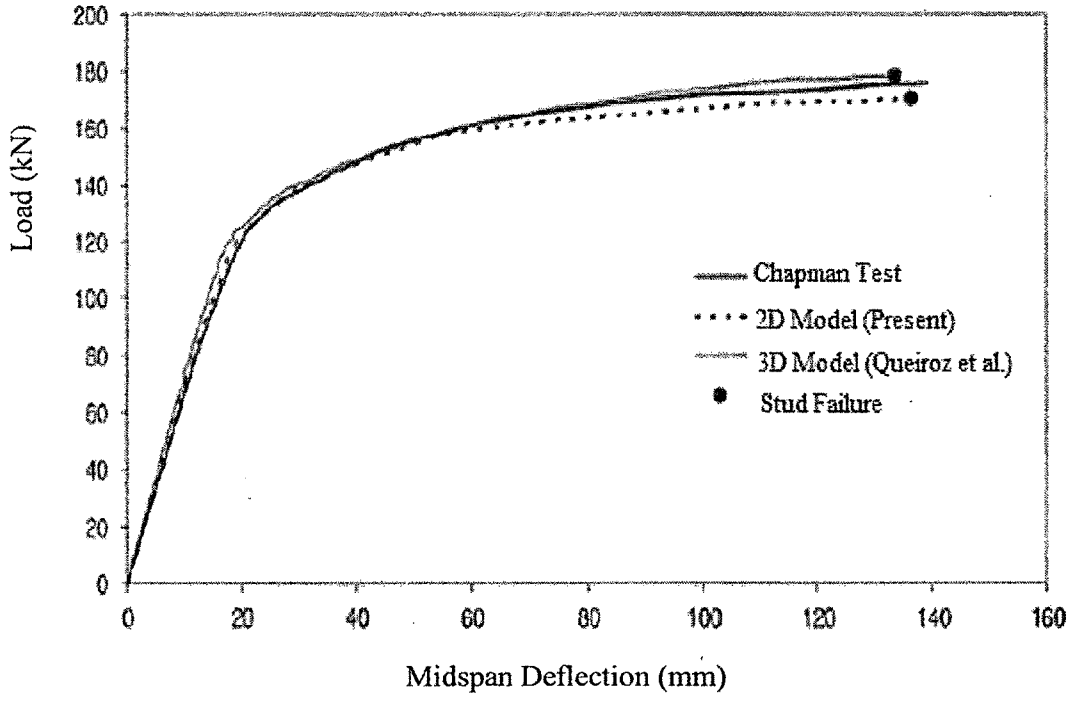

Fig. 12.5 Load versus Mid Span Deflection for Beam U4

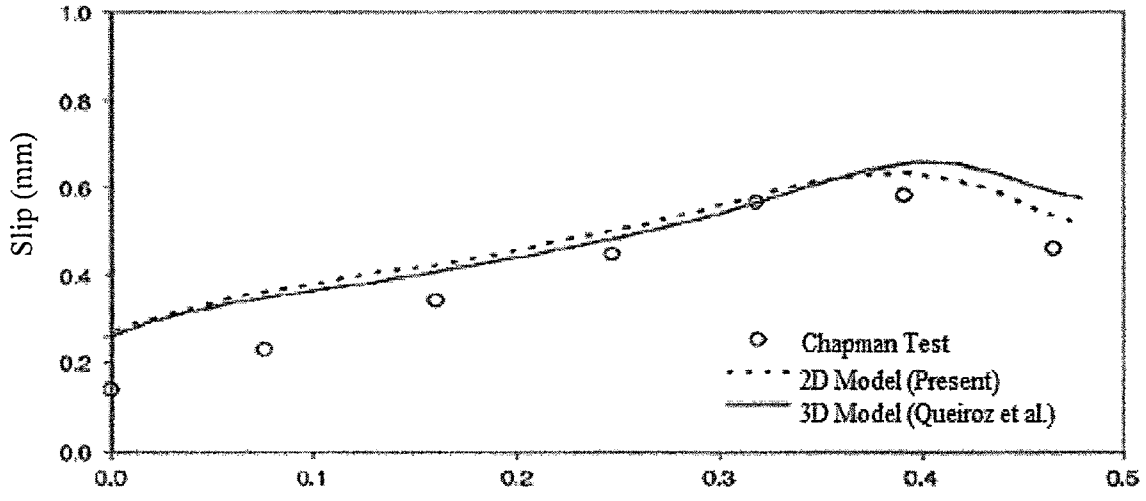

Fig. 12.6 Slip Distribution along Span for Beam E1

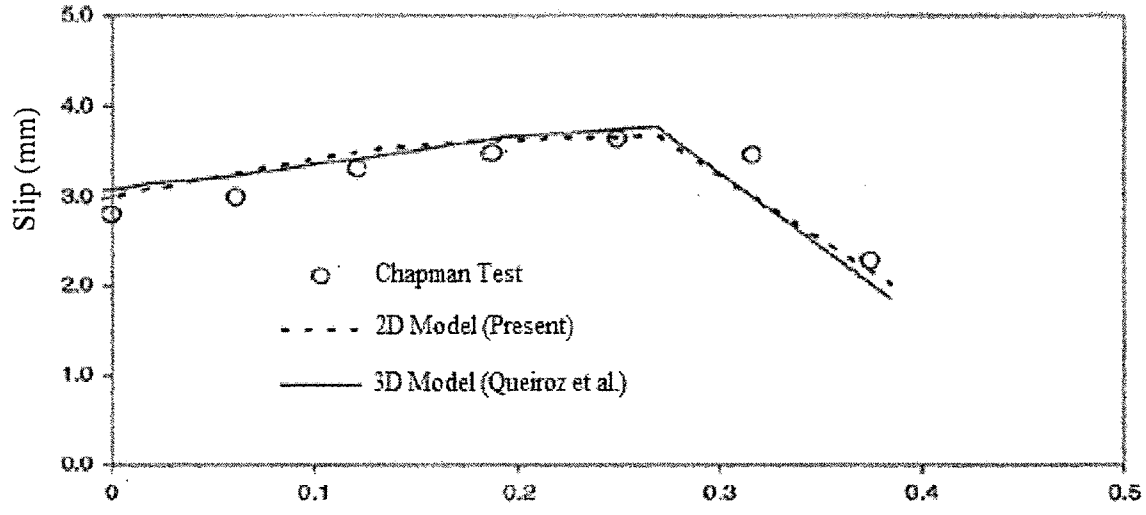

Fig. 12.7 Slip Distribution along Span for Beam U4

It is observed that the present model gives upper bound solution compared to the experimental values. It may be due to the friction between the steel beam-concrete slab interface. Also there may be small differences between the load-slip behaviour of push-off tests given by Chapman and Balakrishnan [14] and the one used in the finite element analysis. **Table 12.2** compares the ultimate load for each of the composite beam studied here.

Table 12.2 Comparison of Ultimate Load Results

Beam Type	$P_{EXP.}$ (kN)	Three Dimensional Model		2D Model
		P_{LB} (kN)	P_{UB}(kN)	P_{UL} (kN)
A2	448	429	469	457
A3	449	425	447	438
A4	523	444	470	410
A5	468	462	479	452
A6	430	-	449	453
B1	486	469	468	470
C1	448	445	474	458
D1	481	457	475	492
E1	513	520	548	538
U1	191	171	178	180
U3	185	166	182	190
U4	176	-	179	195

Figures 12.8 and **12.9** show the results of the FE model for the beams A2 and A5 respectively. Increase in the stiffness of the system is observed. The failure mode of the composite beam changes from slab crushing to slab failure.

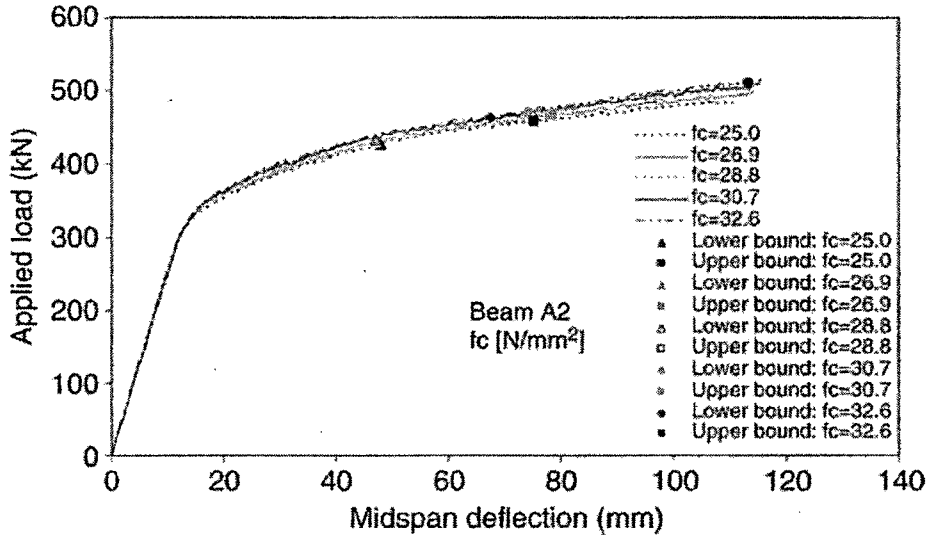

Fig. 12.8 P-Δ for Different Slab Concrete Strengths for Beam A2

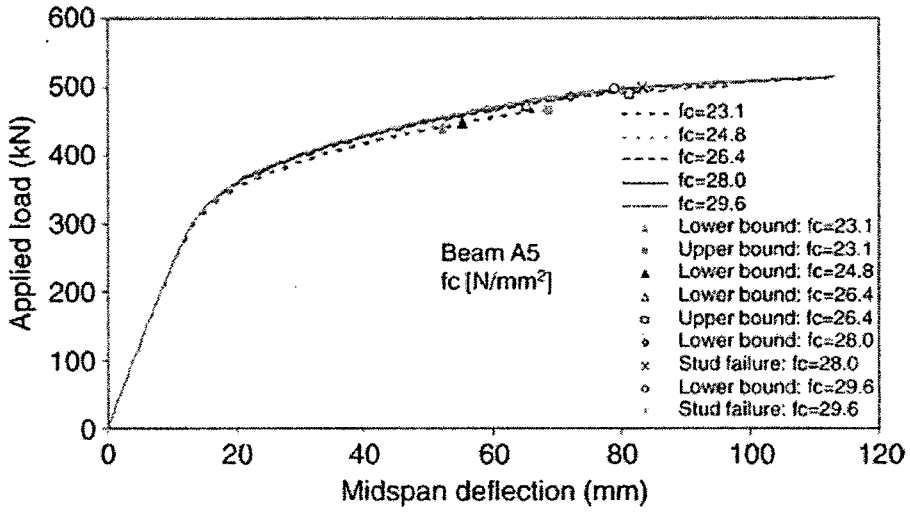

Fig. 12.9 P-Δ for Different Slab Concrete Strengths for Beam A5

12.6 Modelling of Continuous Beam

To verify the FE model in the presence of negative moments, two continuous beams are studied. The beams experimentally tested by Teraszkiewicz [113] are simulated. The test consisted of a composite beam with two spans of 3354 mm, an I-shaped steel beam 152 mm deep and a concrete slab 60 mm thick. The slab was also longitudinally reinforced in the negative moment region (445 mm^2). Stud shear connectors were distributed in pairs at 146 mm pitch along the beam and the structural system was loaded with point loads at mid span. **Fig 12.10** shows the continuous beam. The geometric properties of the beam and the material properties are given in **Tables 12.3** and **12.4** respectively.

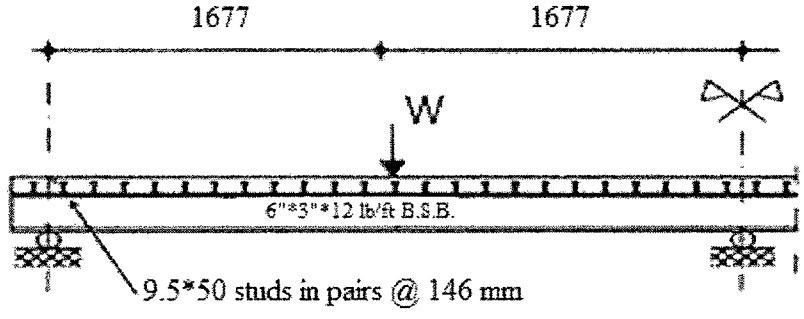

Fig. 12.10 Continuous Composite Beam

The results provided by the FE model and the numerical investigation carried out by Gattesco [44] for the deflected shape and slip along the steel-concrete interface are compared in **Figs. 12.11** and **12.12** respectively.

Table 12.3 Geometric Properties of Composite Beams

Beam Identification		CB1	CTB4
Span Length (mm)		3354	4500
Loading Type		Midspan point load	Midspan point load
Concrete Slab	Thickness (mm)	60	100
	Width (mm)	610	800
Steel Beam	Section	6" x 3" x 12 lb/ft	HEA 200
	Area (mm^2)	2276	5380
Shear Connectors	Kind of stud	9.5 x 50	19 x 75
	Number of studs	96	84
	Pitch of studs (mm)	146	300
Longitudinal Reinforcement	Hogg. (mm^2)	445	804

Table 12.4 Material Properties of Composite Beams

Beam Identification			CB1	CTB4
Concrete	Concrete Strength f_c (MPa)		46.7	34.0
	Tensile Strength f_{ct} (MPa)		3.89	3.15
Steel	Yield Stress (MPa)	Flange	301	236
		Web	321	238
		Reinforcement	470	430
	Ultimate Stress (MPa)	Flange	470	393
		Web	485	401
		Reinforcement	-	533
	Strain Hardening at Strain	Flange	0.012	0.018
		Web	0.012	0.018
		Reinforcement	0.010	0.010

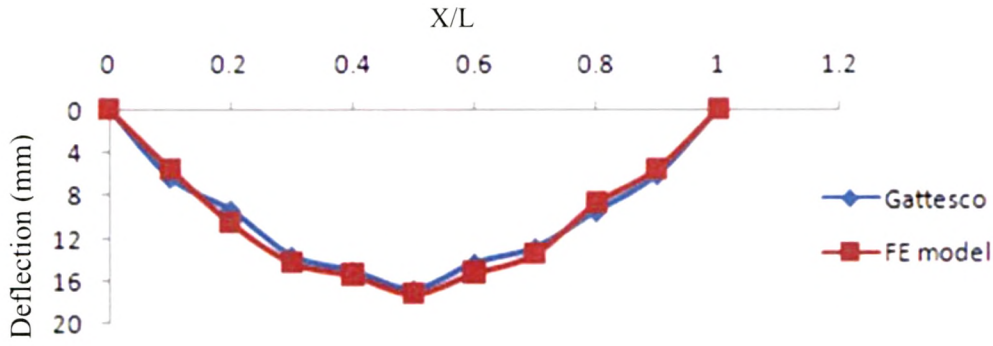

Fig. 12.11 Deflected Shape (X/L = 1, Plane of Symmetry)

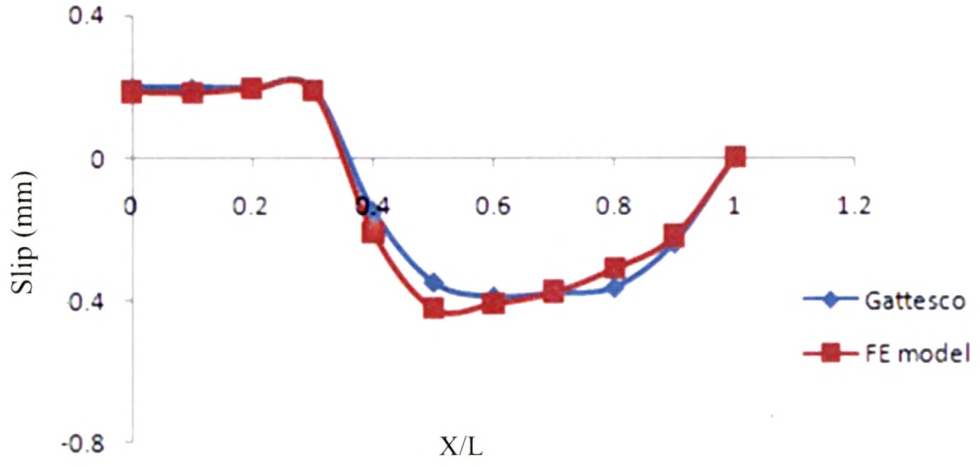

Fig 12.12 Slip Distribution along Span